

# Photoproduction of vector mesons off nucleons near threshold

Bengt Friman

*GSI, Postfach 11 05 52  
D-64220 Darmstadt, Germany  
Institut für Kernphysik, TH Darmstadt  
D-64289 Darmstadt, Germany*

and

Madeleine Soyeur

*Commissariat à l'Energie Atomique  
Laboratoire National Saturne  
CE de Saclay  
F-91191 Gif-sur-Yvette Cedex, France*

---

## Abstract

We propose a simple meson-exchange model of the photoproduction of  $\rho$ - and  $\omega$ -mesons off protons near threshold ( $E_\gamma \lesssim 2\text{ GeV}$ ). This model provides a good description of the available data and implies a large  $\rho$ -nucleon interaction in the scalar channel ( $\sigma$ -exchange). We use this phenomenological interaction to estimate the leading contribution to the self-energy of  $\rho$ -mesons in matter. The implications of our calculation for experimental studies of the  $\rho$ -meson mass in nuclei are discussed.

---

## 1 Introduction

The properties of vector mesons in the nuclear medium appear to be important not only for the understanding of nuclear dynamics but also possibly to reveal a non-perturbative aspect of quantum chromodynamics (QCD), the restoration of chiral symmetry at high baryon density or temperature [1-3].

As a consequence of the spontaneous breaking of chiral symmetry, the QCD vacuum is characterized by a non-zero expectation value, the quark condensate  $\langle \bar{q}q \rangle$ . When the baryon density or temperature increases, this expectation value decreases and would vanish at the critical density or temperature, if chiral symmetry was not explicitly broken by finite quark masses. We consider here the decrease of the quark condensate with increasing density. In the low density approximation, expected to be valid for densities below the saturation density ( $\rho_0$ ), it has been shown that this decrease is linear as a consequence of the Feynman-Hellmann theorem [4,5]. The slope is such that the value of  $\langle \bar{q}q \rangle$  at  $\rho_0$  is about 30% smaller than at  $\rho = 0$ . Observing this effect experimentally is a major challenge.

Brown and Rho [1,6] suggested that the masses of vector mesons ( $\rho$ - and  $\omega$ -mesons) are generated by their repulsive coupling to the quark condensate and therefore decrease with increasing baryon density. In their approach, vector meson masses scale with the cubic root of the quark condensate and have dropped by about 100 MeV at  $\rho_0$ . Decreasing in-medium vector meson masses linked to the decrease of the quark condensate were also obtained by making use of the techniques of QCD sum rules in matter [2,3]. However, this result relies on the factorization of the 4-quark condensate, a possibly questionable approximation. Experimental studies of the in-medium vector meson masses are therefore very much needed and could shed some light on the origin of hadron masses and their relation to chiral symmetry.

The observation of the in-medium behaviour of vector mesons requires processes in which vector mesons are produced and decay inside nuclei. The candidates for such measurements are necessarily broad mesons, as their mean free path has to be shorter than the nuclear size. This is the case for the  $\rho$ -meson which has a total width  $\Gamma_\rho$  of  $(151.2 \pm 1.2)$  MeV and a propagation length  $c\tau_\rho$  of  $\sim 1.3$  fm [7]. The small free space width [7] of the  $\omega$ -meson [ $\Gamma_\omega = (8.43 \pm 0.10)$  MeV and  $c\tau_\omega \simeq 23.4$  fm] precludes such studies, unless  $\omega$ -mesons acquire a large width in matter. It may nevertheless be possible to study the in-medium properties of  $\omega$ -mesons in the particular recoilless kinematics where they are produced approximately at rest in nuclei [8]. We focus on  $\rho$ -mesons and consider their production in nuclear targets close to threshold, where their formation time and lifetime are not dilatated by large Lorentz factors. The spectrum of the corresponding vector excitation can be best studied through its  $e^+e^-$  decay, as the emitted leptons are not distorted by strong interactions. Such experiments are planned at CEBAF [9] and GSI [10].

The main purpose of this work is to construct a model for the photoproduction of  $\rho$ - and  $\omega$ -mesons off protons near threshold ( $E_\gamma \lesssim 2$  GeV) as a first step to study later

their photoproduction in nuclei in that kinematic regime. We show that, close to threshold, the  $\gamma p \rightarrow \omega p$  and the  $\gamma p \rightarrow \rho^0 p$  cross sections [11] can be well described by a simple meson-exchange model. In this picture, the  $\omega$  photoproduction appears dominated by  $\pi$ -exchange while the  $\rho$  photoproduction cross section is given mainly by  $\sigma$ -exchange. Assuming the Vector Dominance of the electromagnetic current [12], we can extract from this last process a phenomenological  $\rho$ -nucleon interaction. We use it to derive the leading contribution to the  $\rho$ -meson self-energy in matter. The  $\rho$ -nucleon interaction in the scalar channel leads to a  $\rho$ -meson self-energy in matter which is large and attractive. We discuss the theoretical interpretation of this effect and its consequences for experimental studies of the  $\rho$ -meson mass in nuclei.

We present our model for the  $\gamma p \rightarrow \omega p$  and  $\gamma p \rightarrow \rho^0 p$  reactions near threshold in Section 2. The  $\rho$ -meson self-energy in matter generated to lowest order by the  $\rho$ -nucleon interaction deduced from this model with the  $\sigma\rho\rho$  coupling we consider is calculated and discussed in Section 3. We conclude by a few remarks in Section 4.

## 2 Vector meson photoproduction off protons near threshold

The production of the  $\rho(770)$ - and  $\omega(782)$ -mesons induced by photons of a few GeV scattered from proton targets has been studied extensively [13]. At sufficiently high energy, typically  $E_\gamma > 3 \text{ GeV}$ , this process appears diffractive: the total cross section is roughly energy independent, the differential cross section  $d\sigma/dq^2$  exhibits a sharp peak in the forward direction, the t-channel exchange has the quantum numbers of the vacuum (Pomeron exchange) and the amplitude is mostly imaginary.

At lower energies ( $E_\gamma < 2 \text{ GeV}$ ), meson-exchange contributions are expected to play a role. The importance of the  $\pi$ -exchange in the  $\gamma p \rightarrow \omega p$  reaction near threshold was emphasized long ago and is supported by data taken with linearly polarized photons [14].

Following the early suggestion of Berman and Drell [15] and work by Joos and Kramer [16], we describe the  $\gamma p \rightarrow V p$  ( $V = \rho^0, \omega$ ) reaction near threshold by t-channel exchanges and assume that the production amplitudes are dominated by the exchange of light mesons. There is no rigorous justification for this choice. We favour this model because it provides a reasonable description of the data with a small number of parameters. It is in particular much simpler than the s-channel picture, based on Compton-like graphs, which requires summation over a very large number of overlapping baryon resonances [17].

For reasons which will become clear later, we begin our discussion by the  $\gamma p \rightarrow \omega p$  reaction. In the Born approximation, only scalar- and pseudoscalar-meson exchanges can contribute to our t-channel description. Vector-meson exchanges are not allowed by charge conjugation invariance. In the pseudoscalar channel, the  $\eta$ -exchange contribution is small compared to the  $\pi$ -exchange for two reasons. First, the total  $\gamma p \rightarrow \omega p$  cross section is dominated by the low  $q^2$  regime, where the  $\eta$ -exchange is strongly

suppressed compared to the  $\pi$ -exchange because of their large mass difference. Second, the  $\omega \rightarrow \eta\gamma$  branching ratio is about two orders of magnitude smaller than the  $\omega \rightarrow \pi^0\gamma$  branching ratio [7]. An explicit calculation shows that the ratio of the coupling constants  $g_{\omega\pi\gamma}^2/g_{\omega\eta\gamma}^2$  is of the order of 15. This implies a further suppression of the  $\eta$ -exchange compared to the  $\pi$ -exchange. Consequently, we are left effectively with two contributions, the  $\pi^0$ -exchange and the  $\sigma$ -exchange shown in Fig. 1.

The relative importance of these two contributions may be assessed by studying the radiative transitions of  $\omega$ -mesons to neutral pions and  $\sigma$ 's. Since the  $\sigma$ -meson is an effective degree of freedom associated with the propagation of two pions in a relative s-wave state, a first estimate of the strength of these transitions can be obtained from the branching ratio of the  $\omega$ -meson into the  $\pi^0\gamma$  and  $\pi^+\pi^-\gamma$  channels (in the latter case, the coupling of the two pions in a  $\rho^0$ -like state is forbidden by charge conjugation invariance). The  $\omega \rightarrow \pi^0\gamma$  branching ratio is known to be of the order of 8.5 % [7]. Unfortunately, the only data available on the  $\omega \rightarrow \pi^+\pi^-\gamma$  branching ratio is an upper limit of  $3.6 \times 10^{-3}$  [7]. This suggests nevertheless that the  $\pi$ -exchange is the dominant contribution. Another approach to evaluate these vertices is Vector Meson Dominance [12]. Because of isospin conservation, the  $\pi^0\omega$  channel will couple only to the isovector part of the electromagnetic current while the  $\sigma\omega$  channel will couple solely to its isoscalar part. Using the current-field identities of Kroll, Lee and Zumino [18], we identify the isoscalar and isovector parts of the electromagnetic current with the  $\omega$ - and  $\rho$ -meson currents respectively. This is shown pictorially in Fig. 2. The relation between the electromagnetic current and the vector fields is given by [18]

$$\mathcal{J}_\mu^{em}(I = 1) = \frac{eM_\rho^2}{2g_\rho}\rho_\mu, \quad (1)$$

$$\mathcal{J}_\mu^{em}(I = 0) = \frac{eM_\omega^2}{2g_\omega}\omega_\mu, \quad (2)$$

where  $M_\rho$  and  $M_\omega$  are the  $\rho$  and  $\omega$ -masses and  $g_\rho$  and  $g_\omega$  are dimensionless constants, which can be determined from the  $e^+e^-$  partial decay widths of the  $\rho$ - and  $\omega$ -mesons [7] to be

$$g_\rho^2 = 6.33 \quad (3)$$

and

$$g_\omega^2 = 72.71. \quad (4)$$

Because the  $\pi^0$ - and  $\sigma$ -mesons have opposite parity, the  $\pi$ - and  $\sigma$ -exchange amplitudes do not interfere. Consequently, the ratio of the  $\pi$ - to  $\sigma$ -exchange contributions to the total  $\gamma p \rightarrow \omega p$  cross section is proportional to  $g_\omega^2/g_\rho^2$ , indicating again the dominance of the  $\pi$ -exchange term. This is consistent with the experimental observation that the exchange of unnatural parity states in the t-channel dominates

the  $\gamma p \rightarrow \omega p$  cross section near threshold [14]. We calculate first the  $\pi$ -exchange contribution to this reaction.

The  $\pi NN$  vertex is described by the pseudoscalar coupling

$$\mathcal{L}_{\pi NN}^{int} = -ig_{\pi NN} \bar{N} \gamma_5 (\vec{\tau} \cdot \vec{\pi}) N \quad (5)$$

with a dipole form factor,

$$F_{\pi NN} = \frac{\Lambda_\pi^2 - m_\pi^2}{\Lambda_\pi^2 - q^2}, \quad (6)$$

where  $m_\pi$  is the pion mass,  $g_{\pi NN}$  the pion-nucleon coupling constant (we take  $g_{\pi NN}^2/4\pi = 14$ ) and  $\Lambda_\pi$  the cut-off characterizing the pion-nucleon vertex. Lorentz and gauge invariances imply that the  $\omega\pi\gamma$  vertex is of the form,

$$\mathcal{L}_{\omega\pi^0\gamma}^{int} = e \frac{g_{\omega\pi\gamma}}{M_\omega} \varepsilon_{\alpha\beta\gamma\delta} \partial^\alpha A^\beta \partial^\gamma \omega^\delta \pi^0, \quad (7)$$

where  $\varepsilon_{\alpha\beta\gamma\delta}$  is the totally antisymmetric Levi-Civita tensor and the dimensional coupling strength has been normalized to the  $\omega$ -meson mass. We use the experimental partial decay width for  $\omega \rightarrow \pi^0\gamma$  [7] to determine the coupling constant  $g_{\omega\pi\gamma}^2 = 3.315$ . Using the current-field identity (1), we can calculate the  $\omega\pi^0\gamma$  vertex assuming  $\rho$ -dominance (as shown in the left graph of Fig. 2) and express the  $\omega\rho^0\gamma$  vertex as a function of the  $\omega\rho^0\pi^0$  interaction. Writing by analogy to (7)

$$\mathcal{L}_{\omega\pi^0\rho^0}^{int} = \frac{g_{\omega\pi\rho}}{M_\omega} \varepsilon_{\alpha\beta\gamma\delta} \partial^\alpha \rho^{0\beta} \partial^\delta \omega^\rho \pi^0, \quad (8)$$

we obtain

$$g_{\omega\pi\rho}^2 = 4g_\rho^2 g_{\omega\pi\gamma}^2 \simeq 84. \quad (9)$$

We fix the non-locality of this vertex from the study of the  $\omega \rightarrow \pi^0\mu^+\mu^-$  form factor analyzed with the interaction Lagrangian (8) and the current-field identity (1). This model of the vertex is shown in Fig. 3 and in Fig. 4 we display the result of the calculated form factor, with a local  $\pi\rho\omega$  vertex (dashed curve) and with an extended vertex of the form  $\Lambda_\rho^2/(\Lambda_\rho^2 - q^2)$  with  $\Lambda_\rho = M_\rho$  (full curve). It is clear that a simple Vector Dominance Model with a local  $\pi\rho\omega$  vertex does not describe the data [19,20] and that an additional form factor is required. We shall not discuss here the theoretical understanding of this vertex [21,22], which is closely related to the non-Abelian anomaly [23]. We assume that the mass scale of the  $\pi\rho\omega$  form factor obtained by studying the Dalitz decay of the  $\omega$ -meson characterizes the size of the  $\pi\rho\omega$  vertex. Consequently, we employ the same value of the cut-off to describe the dependence of the form factor on the pion four-momentum when the  $\rho$ -meson is on-shell and the pion is off-shell.

In this way, all the parameters of our  $\pi$ -exchange model of the  $\gamma p \rightarrow \omega p$  cross section are fixed, except for  $\Lambda_\pi$ , the cut-off mass in the  $\pi$ NN form factor. We determine  $\Lambda_\pi$  from a fit to the total  $\gamma p \rightarrow \omega p$  cross section near threshold ( $E_\gamma^{thr} = 1.108$  GeV), knowing from data that the domain of validity of this pion-exchange model should not extend beyond  $\sim 2$  GeV, as natural parity exchanges (Pomerons) are expected to be responsible for a large fraction of the cross section at  $E_\gamma = 2.8$  GeV [14]. We find that the best fit is obtained for  $\Lambda_\pi = 0.7$  GeV. The total cross section for the  $\gamma p \rightarrow \omega p$  reaction obtained in our model is compared to data [11] in Fig. 5. The  $\pi$ -exchange model accounts for the data below 2 GeV, while for larger photon energies, an additional contribution is needed. The missing cross section is almost independent of energy, a behaviour consistent with the Pomeron-exchange term becoming dominant. The value of  $\Lambda_\pi = 0.7$  GeV is consistent with analyses of pion-nucleon data [24] and with recent work indicating that the larger  $\Lambda_\pi$  obtained in models of the nucleon-nucleon interaction can be reduced if the correlated  $\rho\pi$ -exchange is explicitly included [25].

To have a more stringent test of the form factors, we have calculated with the  $\pi$ -exchange model discussed above the differential cross section  $d\sigma/dq^2$  for the  $\gamma p \rightarrow \omega p$  reaction induced by photons of energies  $1.4 < E_\gamma < 1.8$  GeV. The expression for  $d\sigma/dq^2$  is simply

$$\frac{d\sigma}{dq^2}^{\gamma p \rightarrow \omega p} = \alpha \frac{g_{\pi\rho\omega}^2}{4\pi} \frac{g_{\pi pp}^2}{4\pi} \frac{\pi^2}{4g_\rho^2} \frac{(\hbar c)^2}{M_\omega^2} \frac{1}{E_\gamma^2} \frac{-q^2}{4M_p^2} \left[ \frac{M_\omega^2 - q^2}{m_\pi^2 - q^2} \right]^2 \left[ \frac{\Lambda_\pi^2 - m_\pi^2}{\Lambda_\pi^2 - q^2} \right]^2 \left[ \frac{M_\rho^2 - m_\pi^2}{M_\rho^2 - q^2} \right]^2 \quad (10)$$

and the result of the calculation compared to the data [11] is displayed in Fig. 6.

Within error bars, the general trend of the  $q^2$ -dependence is well reproduced for  $|q^2| < 0.5 \text{ GeV}^2$ . Beyond this value, which corresponds to the range of our cut-offs, we do not expect our model to be valid.

We conclude from this discussion that, sufficiently close to threshold ( $E_\gamma < 2$  GeV), there is no clear indication of anything else contributing to the  $\gamma p \rightarrow \omega p$  process in the t-channel but the  $\pi$ -exchange. It is also remarkable that for values of the coupling constants and the cut-offs consistent with other processes, the total cross section is correctly given by this simple model.

Motivated by this result, we study the  $\gamma p \rightarrow \rho^0 p$  reaction within the same approach. As in the case of  $\omega$  photoproduction, vector-meson exchanges are not allowed and we consider only the  $\pi^0$ - and  $\sigma$ -exchanges shown in Fig. 7. Only the isoscalar part of the electromagnetic current ( $\omega$  field) contributes to the  $\pi$ -exchange graph, while the  $\sigma$ -exchange selects the isovector part ( $\rho^0$  field).

In contrast to what happens in the  $\omega$  photoproduction, the scalar-exchange appears to be the dominant contribution to the  $\gamma p \rightarrow \rho^0 p$  reaction. We see two reasons for

this. Information on the scalar and pseudoscalar coupling strengths can be inferred from an analysis of the  $\rho^0$  radiative decays. In spite of unfavourable phase space, the  $\rho^0 \rightarrow \pi^+\pi^-\gamma$  branching ratio of  $(9.9 \pm 1.6) \times 10^{-3}$  is an order of magnitude larger than the  $\rho^0 \rightarrow \pi^0\gamma$  branching ratio of  $(7.9 \pm 2.0) \times 10^{-4}$  [7] (again the  $\rho^0$ -like coupling of the  $\pi^+\pi^-$  pair in the  $\rho^0 \rightarrow \pi^+\pi^-\gamma$  decay is forbidden by charge conjugation invariance). Using the current-field identities (1)-(2), it is also clear from Fig. 7 that the  $g_\omega^2/g_\rho^2$  ratio of  $\sim 10$  is now in favour of the  $\sigma$ -exchange contribution to the cross section.

We keep both  $\pi$ - and  $\sigma$ -exchanges in the calculation of the  $\gamma p \rightarrow \rho^0 p$  cross section. The  $\pi$ -exchange contribution is evaluated with the same parameters as those used for the description of the  $\gamma p \rightarrow \omega p$  cross section. The  $\sigma$ -exchange involves two vertices. We describe the  $\sigma NN$  vertex by the scalar coupling,

$$\mathcal{L}_{\sigma NN}^{int} = g_{\sigma NN} \bar{N} N \sigma, \quad (11)$$

with the form factor

$$F_{\sigma NN} = \frac{\Lambda_\sigma^2 - m_\sigma^2}{\Lambda_\sigma^2 - q^2}. \quad (12)$$

The  $\sigma$  mass  $m_\sigma$  is taken to be 500 MeV as the  $\sigma$ -meson introduced here should be viewed as representing the exchange of two uncorrelated as well as two resonating pions. For the coupling constant, we use the standard value  $g_{\sigma NN}^2/4\pi = 8$  [26]. The cut-off  $\Lambda_\sigma$  will be determined later. By analogy to the  $\omega\pi^0\rho^0$  vertex, we construct first the  $\rho^0\sigma\rho^0$  vertex guided by the current-field identities (1)-(2),

$$\mathcal{L}_{\rho^0\sigma\rho^0}^{int} = \frac{g_{\sigma\rho\rho}}{M_\rho} \left[ \partial^\alpha \rho^{0\beta} \partial_\alpha \rho_\beta^0 - \partial^\alpha \rho^{0\beta} \partial_\beta \rho_\alpha^0 \right] \sigma, \quad (13)$$

and use a  $\sigma\rho\rho$  form factor of the monopole form  $(\Lambda_{\sigma\rho\rho}^2 - m_\sigma^2)/(\Lambda_{\sigma\rho\rho}^2 - q^2)$ . We then fit the values of  $\Lambda_\sigma$ ,  $\Lambda_{\sigma\rho\rho}$  and  $g_{\sigma\rho\rho}$  to data.

The important constraints on the vertices come from the differential cross section  $d\sigma/dq^2$  given as the sum of  $\pi$ - and  $\sigma$ -exchanges by

$$\begin{aligned}
\frac{d\sigma^{\gamma p \rightarrow \rho^0 p}}{dq^2} = & \alpha \frac{g_{\pi\rho\omega}^2}{4\pi} \frac{g_{\pi pp}^2}{4\pi} \frac{\pi^2}{4g_\omega^2} \frac{(\hbar c)^2}{M_\omega^2} \frac{1}{E_\gamma} \frac{-q^2}{4M_p^2} \left[ \frac{M_\rho^2 - q^2}{m_\pi^2 - q^2} \right]^2 \left[ \frac{\Lambda_\pi^2 - m_\pi^2}{\Lambda_\pi^2 - q^2} \right]^2 \\
& + \alpha \frac{g_{\sigma\rho\rho}^2}{4\pi} \frac{g_{\sigma pp}^2}{4\pi} \frac{\pi^2}{4g_\rho^2} \frac{(\hbar c)^2}{M_\rho^2} \frac{1}{E_\gamma} \frac{4M_p^2 - q^2}{4M_p^2} \left[ \frac{M_\rho^2 - q^2}{m_\sigma^2 - q^2} \right]^2 \\
& \left[ \frac{\Lambda_\sigma^2 - m_\sigma^2}{\Lambda_\sigma^2 - q^2} \right]^2 \left[ \frac{\Lambda_{\sigma\rho\rho}^2 - m_\sigma^2}{\Lambda_{\sigma\rho\rho}^2 - q^2} \right]^2. \tag{14}
\end{aligned}$$

We find that the total  $\gamma p \rightarrow \rho p$  cross section for  $E_\gamma < 2$  GeV and the differential cross section  $d\sigma/dq^2$  for  $1.4 < E_\gamma < 1.8$  GeV are well reproduced for  $\Lambda_\sigma = 1$  GeV,  $\Lambda_{\sigma\rho\rho} = 0.9$  GeV and  $g_{\sigma\rho\rho}^2/4\pi = 14.8$ . The calculated curves are compared to data [11] in Figs. 8 and 9.

The data points for the total cross section are very much spread, reflecting the uncertainties in extracting the  $\rho$ -meson production cross section from the  $\pi^+\pi^-$  pair emission [11]. Better data are very much needed. In view of this, there is a large uncertainty in the fit. Nevertheless, it is clear that our  $(\pi + \sigma)$ -exchange model is below the data for  $E_\gamma > 2$  GeV, as expected. It would be important to determine the  $\rho$  photoproduction cross section between 1.5 and 2 GeV better to find out where it becomes diffractive. We should remark that we use a zero-width description of the produced  $\rho$ -meson. This is in general a good approximation for the quantities we calculate, in particular since we do not consider cross sections in a specific  $\rho$  decay channel. However, in the zero-width approximation, we cannot reproduce the lowest energy point ( $E_\gamma = 1.05$  GeV), which is below “threshold”.

As shown in Fig. 9, the  $\pi$ -exchange contributes very modestly to the cross section, at any momentum transfer. The differential cross section provides definite constraints on the cut-offs and couplings for the  $\sigma$ -exchange. In the total cross section, there is a trade-off between the form factors and the  $\sigma\rho\rho$  coupling strength. However, increasing the cut-off masses to compensate for a smaller value of  $g_{\sigma\rho\rho}$  would produce a differential cross section which is too flat.

The  $\rho^0\sigma\rho^0$  vertex (13), suggested by current-field identities, is not unique. Lorentz invariance allows also for a nonderivative coupling of the form,

$$\mathcal{L}_{\rho^0\sigma\rho^0}^{int} = \frac{1}{2} \tilde{g}_{\rho\rho\sigma} M_\rho \rho^\mu \rho_\mu \sigma. \tag{15}$$

This vertex used in the calculation of the photoproduction cross section leads however to a result which is not gauge invariant. Hence, we do not consider it in this work.

The phenomenological T-matrix for the  $\rho$ -nucleon interaction, obtained in the Born approximation, fits the available data on the  $\gamma p \rightarrow \rho^0 p$  reaction near threshold. In the following section we employ this interaction to derive the  $\rho$ -meson self-energy in the nuclear medium.



### 3 The $\rho$ -meson self-energy in matter

To leading order, the  $\rho$ -meson self-energy in nuclear matter is given by the tadpole diagram shown in Fig. 10. This is, in the Born approximation, nothing but the low-density theorem discussed in Ref. [27]. We calculate this term with  $\sigma\rho^0$  coupling given by Eqs. (13). The corresponding self-energy is denoted by  $\Sigma_\rho$ . We find

$$\Sigma_\rho(q^2) = -\frac{g_{\sigma\rho\rho}}{M_\rho} \frac{g_{\sigma NN}}{m_\sigma^2} \frac{\Lambda_\sigma^2 - m_\sigma^2}{\Lambda_\sigma^2} \frac{\Lambda_\rho^2 - m_\sigma^2}{\Lambda_\rho^2} q^2 \rho, \quad (16)$$

where  $q$  is the  $\rho$ -meson 4-momentum and  $\rho$  is the matter density. Using the parameters obtained in the previous section, we get

$$\Sigma_\rho(q^2) \simeq -2.81 q^2 \rho (fm^{-3}) GeV^2. \quad (17)$$

We have assumed that the a priori unknown phase of the  $g_{\sigma\rho\rho}$  coupling constant is such that the corresponding self-energy is attractive. This follows naturally if we think of the  $\sigma$ -exchange as an effective  $2\pi$ -exchange process where the intermediate states are dominated by states of energies higher than the  $\rho$  mass. An example of such a process with an intermediate  $\omega$  particle-hole state is shown in Fig. 11b.

The corresponding in-medium inverse  $\rho$ -meson propagator is

$$D_\rho^{-1}(q^2) = D_\rho^{0-1} - \Sigma_\rho, \quad (18)$$

with  $D_\rho^{0-1} = q^2 - M_\rho^2$ . From Eqs. (17), we obtain

$$D_\rho^{-1}(q^2) = q^2 [1 + 2.81 \rho (fm^3)] - M_\rho^2. \quad (19)$$

With the derivative  $\sigma\rho$  coupling of Eq. (13), the self-energy gives rise to a wave function renormalization. Equation (19) can indeed be written as

$$D_\rho(q^2) = \frac{Z}{q^2 - ZM_\rho^2 + i\varepsilon} \quad (20)$$

with

$$Z^{-1} = 1 + \frac{g_{\sigma\rho\rho}}{M_\rho} \frac{g_{\sigma NN}}{m_\sigma^2} \frac{\Lambda_\sigma^2 - m_\sigma^2}{\Lambda_\sigma^2} \rho = 1 + 2.81 \rho (fm^{-3}). \quad (21)$$

At  $\rho = \rho_0$ , the pole is shifted down from  $M_\rho$  to  $0.82 M_\rho$  and the strength is reduced by 32 %. This result may at first sight seem dubious, since the total strength satisfies

a sum rule

$$\int \frac{dq^2}{\pi} [-\text{Im}D_\rho(q^2)] = 1. \quad (22)$$

This can be understood by considering the underlying picture where the  $\sigma$ -exchange effectively accounts for a  $2\pi$ -exchange process (see Fig. 11a). The associated  $\rho$ -meson self-energy (Fig. 11b) is energy-dependent and has an imaginary part. In the case illustrated in Fig. 11b, it corresponds to the decay of a  $\rho$ -meson (off-shell) into an  $\omega$ -meson and a particle-hole pair. This physical process also shows up in the analytical structure of the  $\rho$  propagator as a cut in the complex  $q^2$  plane. By replacing the  $2\pi$ -exchange effectively by a  $\sigma$ -exchange, one implicitly assumes that this cut is far away from the energies of interest, so that the energy dependence due to the intermediate states can be neglected. For the problem at hand, this assumption is not rigorously justified. In what follows, we shall however assume that the dominant contributions to the intermediate states have masses larger than the  $\rho$ -meson mass.

To see how this picture affects the sum rule, let us consider the following schematic model. Replace the cut in the self-energy by a simple pole located at  $q^2 = M^2$ . The  $\rho$ -meson self-energy is then of the form

$$\Sigma_\rho(q^2) = f^2 q^2 \frac{M^2}{q^2 - M^2}. \quad (23)$$

We assume derivative coupling so that the self-energy is proportional to  $q^2$ . Thus, the self-energy (23) reduces to the  $\sigma$ -induced self-energy (16) in the limit  $M \rightarrow \infty$ .

The propagator

$$D_\rho(q^2) = \frac{1}{q^2 - M_\rho^2 - \Sigma_\rho(q^2)} \quad (24)$$

has two poles, a low mass one  $q_A^2$  near  $M_\rho^2$ , and a high mass one  $q_B^2$  near  $M^2$ . The low mass pole is identified with the in-medium  $\rho$ -meson. For  $M \gg M_\rho$ , one finds, to leading order in  $(M_\rho/M)^2$ ,  $q_A^2 = M_\rho^2/(1+f^2)$  and  $q_B^2 = (1+f^2)M$ . The corresponding residues are  $Z_A = 1/(1+f^2)$  and  $Z_B = f^2/(1+f^2)$  and the sum rule is fulfilled, i.e.,  $Z_A + Z_B = 1$ . In the limit  $M \rightarrow \infty$ ,  $q_B^2 \rightarrow \infty$  but  $Z_B$  remains finite. The missing strength is moved out to  $q^2 = \infty$ . Consequently, the propagator (20) does not satisfy the sum rule because it is valid only at low energies, while the sum rule involves all energies. Thus, our choice of phases for the coupling constants, which leads to a reduced  $\rho$ -mass in medium, is consistent also with the sum rule (22).

## 4 Concluding remarks

We have shown in this paper that the presently available data on the photoproduction of  $\rho$ - and  $\omega$ -mesons off protons near threshold ( $E_\gamma < 2$  GeV) can be well described by a simple one-boson-exchange model. The dominant processes are the pseudoscalar  $\pi$ -exchange for the  $\omega$  photoproduction and the scalar exchange, which we parametrize by an effective  $\sigma$ -meson, for the  $\rho^0$  photoproduction.

The  $\pi$ -exchange model of the  $\gamma p \rightarrow \omega p$  is constructed using parameters constrained by other data with moderate extrapolations. We rely however on the measurement of the  $\omega \rightarrow \pi^0 \mu^+ \mu^-$  form factor for values of the invariant  $\mu^+ \mu^-$  pair mass of the order of 500 to 600 MeV (close to the  $\rho$  pole). These data [19,20] have large error bars and have been obtained with very few events. A better measurement of this form factor appears very important for the understanding of the  $\omega \pi^0 \gamma^*$  vertex, in which  $\gamma^*$  is a virtual time-like photon. It is interesting that both our  $\pi$ -exchange model and polarization data [14] on the  $\gamma p \rightarrow \omega p$  reaction close to threshold do not seem to require a scalar exchange. This suggests that the  $\sigma \omega$  interaction is substantially weaker than the  $\sigma \rho$  interaction.

The  $(\pi + \sigma)$ -exchange model of the  $\gamma p \rightarrow \rho^0 p$  reaction is much less constrained and it is clear that it does not provide a detailed understanding of the photoproduction of  $\rho$ -mesons near threshold. It is indeed desirable to build a dynamical model of the effective  $\sigma$ -exchange, going beyond the Born approximation, to unravel the physics of this process. This will make it possible to determine the important contributions to the intermediate states of the type shown in Fig. 11b and put our discussion of Section 3 on a firmer basis. Such a dynamical model would also allow a consistent discussion of the  $\sigma \rho$  and  $\sigma \omega$  vertices. It could provide a more detailed comparison to data through a study of the energy-dependence of the ratio of the real to the imaginary parts of the production amplitude, a quantity expected to be very sensitive to the underlying dynamics. Work in this direction is in progress. We also reemphasize the need for much more accurate data than those presently available [11].

Our discussion of the  $\rho$ -meson self-energy in matter shows the importance of the structure of the  $\sigma \rho$  vertex. The off-shell behaviour plays a very important role in determining this self-energy from the  $\rho^0$  photoproduction reaction. Additional constraints on the  $\sigma \rho$  vertex from different kinematic regimes (available for example in the electroproduction of vector mesons near threshold) would be very important to establish our result on a more solid basis. Systematic studies of processes involving vector mesons in a consistent theoretical framework, such as nonlinear chiral Lagrangians in which vector mesons are introduced as dynamical gauge bosons [28], could also provide useful guidance for choosing the form of the interaction vertices. The particular form of the  $\rho$ -meson self-energy will affect the dilepton spectrum of  $\rho$ -like excitations in nuclei. The theoretical interpretation of this spectrum is therefore closely linked to the understanding of the momentum dependence of the  $\rho$  self-energy at finite baryon density.

## 5 Acknowledgements

We thank George Bertsch, Mannque Rho and Wolfram Weise for very helpful discussions. One of us (M. S.) acknowledges the generous hospitality of GSI, where part of this work was done.

## References

- [1] G.E. Brown and M. Rho, Phys. Rev. Lett. 66 (1991) 2720
- [2] T. Hatsuda and S.H. Lee, Phys. Rev. C46 (1992) R 34
- [3] M. Asakawa and C.M. Ko, Nucl. Phys. A560 (1993) 399; Phys. Rev. C48 (1993) R526
- [4] T.D. Cohen, R.J. Furnstahl and D.K. Griegel, Phys. Rev. C45 (1992) 1881
- [5] M. Lutz, S. Klimt and W. Weise, Nucl. Phys. A542 (1992) 621
- [6] G.E. Brown and M. Rho, to be published in Physics Reports
- [7] Review of Particle Properties, Phys. Rev. D50 (1994) 1173
- [8] HADES Collaboration, private communication
- [9] CEBAF Proposal PR 89-001, Nuclear mass dependence of vector mesons using the photoproduction of lepton pairs, Spokesmen: D. Heddle and B.M. Preedom; CEBAF Proposal PR 94-002, Photoproduction of vector mesons off nuclei, Spokesmen: P.Y. Bertin, M. Kossov and B.M. Preedom
- [10] HADES Proposal, GSI Internal Report
- [11] Aachen-Berlin-Bonn-Hamburg-Heidelberg-München Collaboration, Phys. Rev. 175 (1968) 1669
- [12] M. Gell-Mann and F. Zachariasen, Phys. Rev. 124 (1961) 953; J.J Sakurai, Currents and Mesons, The University of Chicago Press, 1969
- [13] D.W.G.S. Leith, in Electromagnetic Interactions of Hadrons, edited by A. Donnachie and G. Shaw (Plenum, New-York), Vol. I (1978) 345
- [14] G. Wolf, in the Proceedings of the 1971 International Symposium on Electron and Photon Interactions at High Energies, Cornell University, Ithaca (USA), August 23-27, 1971, p. 190
- [15] S.M. Berman and S.D. Drell, Phys. Rev. 133 (1964) 3791
- [16] H. Joos and G. Kramer, Z. Physik 178 (1964) 542
- [17] M. Schäfer, M.C. Dönges and U. Mosel, Phys. Lett. B342 (1995) 13
- [18] N.M. Kroll, T.D. Lee and B. Zumino, Phys. Rev. 157 (1967) 1376
- [19] R.I. Dzhelyadin et al, Phys. Lett. B 102 (1981) 296
- [20] L.G. Landsberg, Phys. Rep. 128 (1985) 30
- [21] V. Theileis, Diplomarbeit, Institut für Kernphysik, Technische Hochschule Darmstadt (1995) and to be published
- [22] F. Klingl, Diplomarbeit, Institut I - Theoretische Physik, Universität Regensburg (1995) and to be published

- [23] T. Fujiwara *et al.*, Prog. Theor. Phys. 73 (1985) 926
- [24] S.A. Coon and M.D. Scadron, Phys. Rev. C23 (1981) 1150; C42 (1990) 2256; A.W. Thomas and K. Holinde, Phys. Rev. Lett. 63 (1989) 2025
- [25] G. Janssen *et al.*, Phys. Rev. Lett. 71 (1993) 1978
- [26] R. Machleidt, Adv. in Nucl. Phys. 19 (1989) 189
- [27] C.B. Dover, J. Hüfner and R.H. Lemmer, Ann. Phys. 66 (1971) 248; M. Lutz, A. Steiner and W. Weise, Nucl. Phys. A574 (1994) 755
- [28] M. Bando *et al.*, Phys. Rev. Lett. 54 (1985) 1215

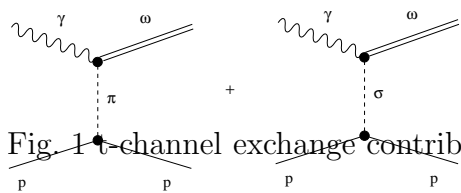
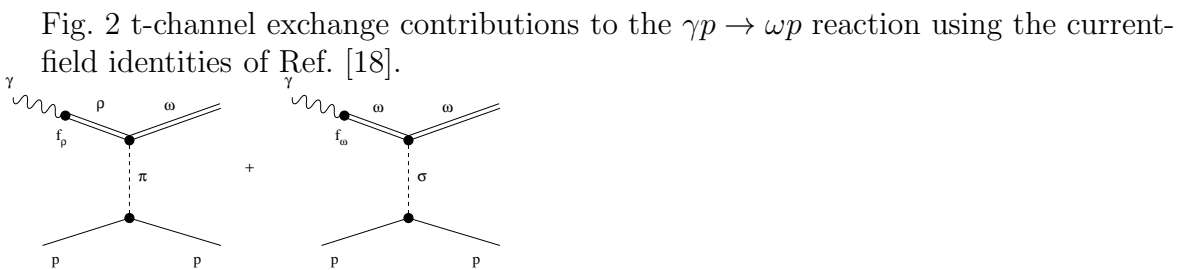


Fig. 1 t-channel exchange contributions to the  $\gamma p \rightarrow \omega p$  reaction.



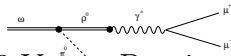


Fig. 3 Vector Dominance Model of the  $\omega$  Dalitz decay form factor.

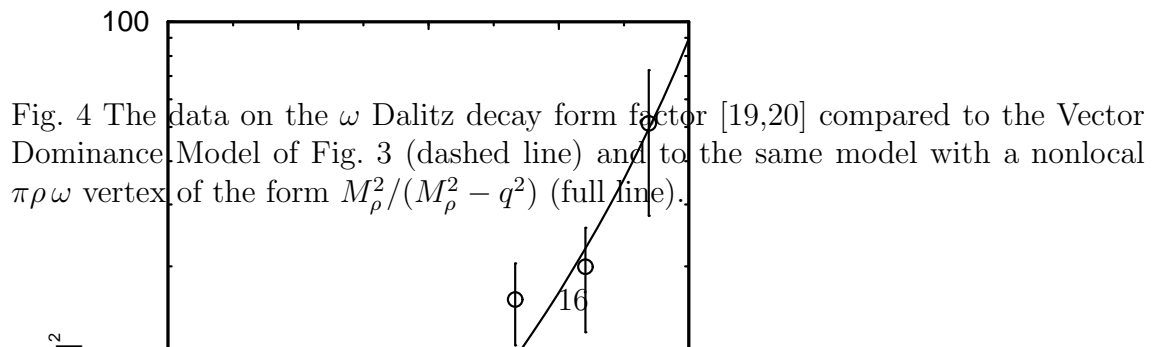




Fig. 5 Energy dependence of the  $\pi$ -exchange model of the  $\gamma p \rightarrow \omega p$  total cross section. The data are from Ref. [11], where the meaning of the different sets of data points is explained.

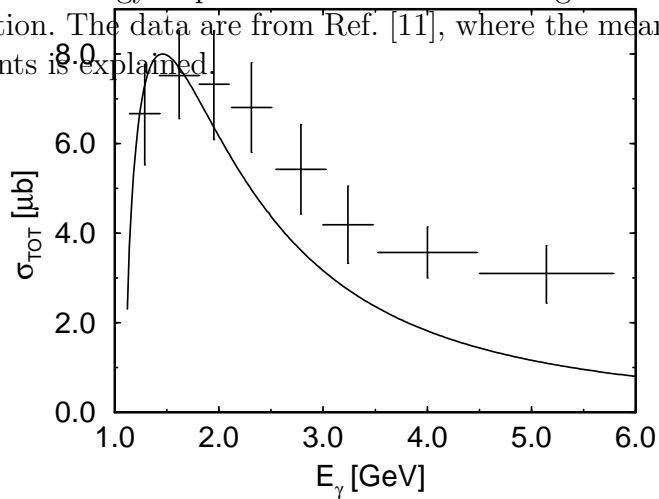
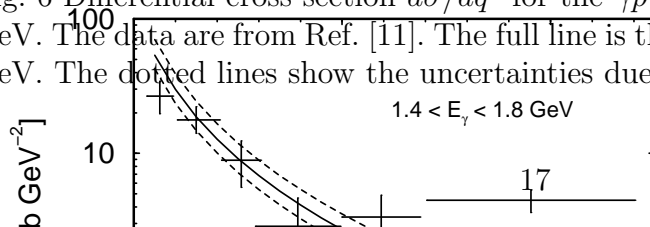


Fig. 6 Differential cross section  $d\sigma/dq^2$  for the  $\gamma p \rightarrow \omega p$  reaction at  $1.4 < E_\gamma < 1.6$  GeV. The data are from Ref. [11]. The full line is the  $\pi$ -exchange model for  $E_\gamma = 1.6$  GeV. The dotted lines show the uncertainties due to the photon energy resolution



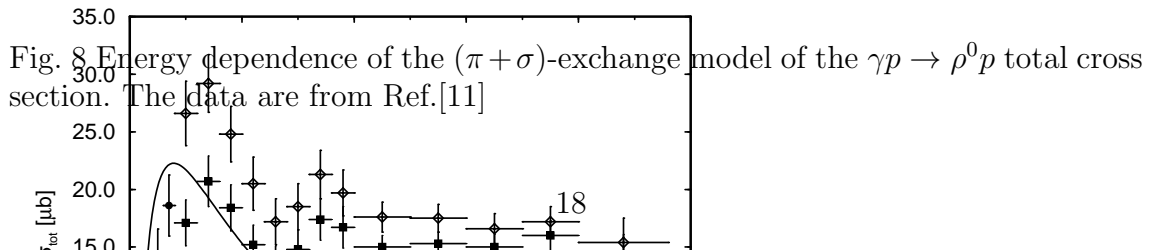
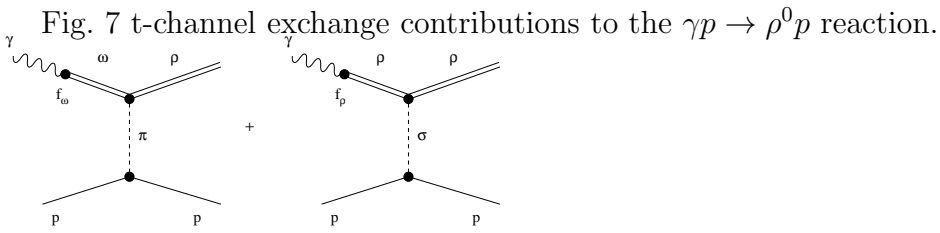


Fig. 9 Differential cross section  $d\sigma/dq^2$  for the  $\gamma p \rightarrow \rho^0 p$  reaction. The data are from Ref. [1]. The full line is the  $(\pi + \sigma)$ -exchange model for  $E_\gamma = 1.6$  GeV. The dot-dashed line shows the  $\pi$ -exchange contribution. The dotted lines show the uncertainties due to the photon energy resolution.

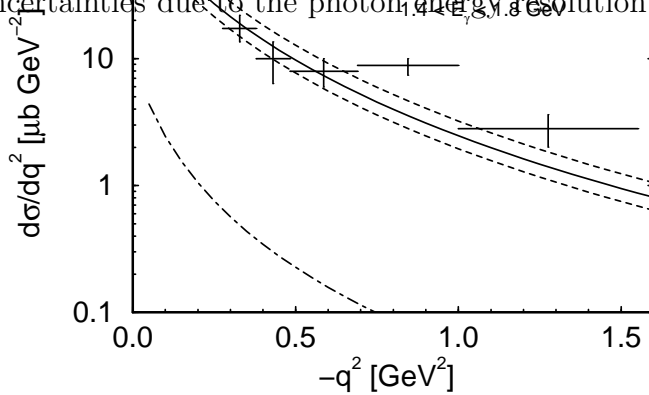


Fig. 10 The  $\rho$ -meson self-energy in matter to lowest order in the density.

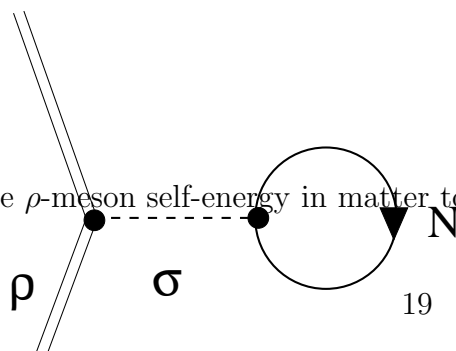
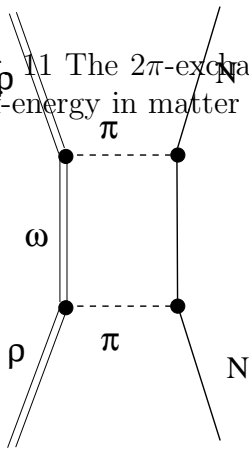
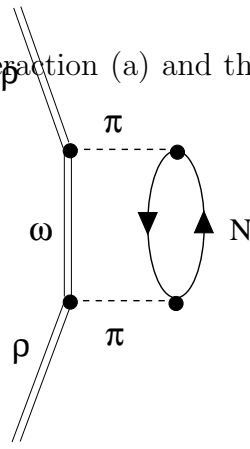


Fig. 11 The  $2\pi$ -exchange  $\rho$ -nucleon interaction (a) and the corresponding  $\rho$ -meson self-energy in matter (b).



a



b